Estimation of Atmospheric Moisture Content from Microwave Radiometric Measurements during CCOPE

BJORN H. LAMBRIGTSEN

Institute for Atmospheric Optics and Remote Sensing, Hampton, VA 23666

RAMESH K. KAKAR

Earth and Space Sciences Division, Jet Propulsion Laboratory, California Institute of Technology, Pasadena, CA 91109

(Manuscript received 30 April 1984, in final form 13 November 1984)

ABSTRACT

We have applied a multiple linear regression technique to retrieve continuous sequences of atmospheric moisture profiles from a set of measured data. In this method the selection of an optimal subset of sensor channels plays a crucial role, in order to reduce the impact of data noise and redundancy. The data were obtained with a 4-channel remote-sensing microwave instrument carried aboard an aircraft. In contrast, most previously reported moisture profile retrievals from microwave radiometry have been used on simulated, discontinuous data. Although our data were obtained over a land surface with only a limited amount of correlative data, the retrievals were quite successful.

1. Introduction

To understand the physical processes involved in convective storm lifetimes, a Cooperative Convective Precipitation Experiment (CCOPE) was carried out in 1981. The experiment was performed over a 3-month period at a site in Eastern Montana. An Advanced Microwave Moisture Sounder (AMMS) was flown on a NASA aircraft as part of the CCOPE between 28 May and 11 June 1981 over the mountainous terrain of southeast Montana. A description of aircraft observations obtained with the AMMS during CCOPE and a discussion of the instrument and its method of calibration is given by Krupp and Nieman (1982).

One of the main objectives of AMMS participation was to test water-vapor profile retrieval techniques in clear and slightly cloudy conditions. A number of coincident radiosonde measurements provided a good opportunity to test the remote sensing techniques. In this paper we have presented the results of a statistical correlation method to retrieve continuous sequences of atmospheric moisture profiles from a subset of AMMS measurements during the CCOPE.

2. Retrieval algorithm

The statistical retrieval algorithm has been described in some detail in an earlier paper in which it was applied to simulated retrievals of water vapor profiles (Kakar and Lambrigtsen, 1984). In this method the amount of water vapor $q(p)$ at a pressure level p is given by

$$q(p) = a(p) + \sum_{i=1}^{N} b_i(p) T_b(\nu_i), \qquad (1)$$

where N is the number of available radiometer channels, $a(p)$ and $b_i(p)$ are regression coefficients and $T_b(\nu_i)$ is the measured channel brightness temperature at frequency ν_i. Optimum subsets of the N channels are used at every pressure level for the retrieval of water vapor. These optimum channel subsets are obtained by the application of the method of "regressions by leaps and bounds" (Furnival and Wilson, 1974).

Three categories of data are required to perform the three distinct functions of preparing for, carrying out and testing the quality of the retrievals. First of these is a data base consisting of measured moisture and temperature profiles (from radiosondes) which are representative of the general area and time span of interest. In lieu of exactly coincident measured brightness temperatures, the latter are simulated by performing radiative transfer calculations based on these profiles. We shall refer to the resulting set of moisture profiles and computed brightness temperatures as the statistical data base, since it is used to derive the regression coefficients, $a(p)$ and $b_i(p)$. A set of candidate channel subsets is thus determined, one of each size from one channel to the total number of channels available (here, 8). Each such subset is the best of its size; i.e., it represents the highest correlation between q and T_b in the statistical data set. Among these candidate subsets, there is normally one which

is optimal for retrievals from a particular set of measured T_b. The choice of this optimal subset depends on the measured T_b data to which it is to be applied and not on the statistical data base from which it was derived. It represents a compromise between the conflicting effects of gaining additional information (as reflected in a higher statistical correlation) and increasing the number of noise sources in the retrieval equation as the subset size is increased. Our selection method consists in performing a test retrieval and comparing it with an appropriate measured moisture profile using each subset in turn, and then choosing the subset which gives the best agreement.

The second data set contains the measured brightness temperatures, which are used exclusively to compute all retrievals.

The third data set is the correlative, or reference, data set and consists of *in situ* measurements of moisture coincident in time and space with the remotely sensed brightness temperatures of the second data set. Because of the scarcity of such data, we have used it for several purposes. The primary use is as a reference to compare retrieved and true profiles. Second, part of it is used to select an optimal channel subset, as described above. Finally, a small part of it is also used to "calibrate" the radiative transfer computations used to derive the brightness temperatures of the statistical data base by compensating for systematic computational and other errors. This is discussed in further detail in Section 3.

3. Data sets

a. AMMS data and coincident radiosondes

During CCOPE, the 4-channel AMMS (comprising a 92 GHz window channel and three water absorption channels at 183 ± 2, ±5, ±9 GHz) was periodically operated in "stare" mode (rather than the normal left-to-right scan mode), in which 150 consecutive nadir-looking T_b were obtained, immediately followed by 150 consecutive 45°-right-looking ones. Each 150-pixel sequence lasts for approximately 23 seconds and covers a ground area of approximately 0.3 km × 2 km (nadir) for the 183 GHz channels and twice as wide for the window channel. This high concentration of data in both time and space permits a substantial reduction of noise through averaging. These 150-pixel averages constitute our measured data for, in effect, eight channels (four nadir, four right).

Moisture data for reference and data base use can be derived from radiosondes which were periodically released from five ground stations in the area. We have used 50 sondes for the statistical data base, covering five days. Our objective was to test the retrieval method under stable and cloud-free conditions. Although such conditions did not generally prevail during CCOPE, 11 June comes closest. We have chosen some of the 11 June AMMS data to test our retrievals. Of the 50 radiosondes mentioned here, 15 covering 11 June therefore were used to check the validity of the retrievals.

The 11 June AMMS and radiosonde data used by us is shown in Figs. 1–4:

- Figure 1 is a navigation map showing the 11 June flight tracks (each labeled with a flight track number). Each stare mode sequence is indicated by a tick mark and the corresponding time (GMT). Radiosonde stations are marked with solid circles.
- Figure 2 shows sequentially measured T_b data (150-pixel averages) at the times and locations indicated on the navigation map, together with corresponding ground elevation data (extracted from USGS topographic maps). The result of normalizing window channel T_b to a 920 mb reference elevation of 782 m (see below) is shown as broken lines.
- Figure 3 shows radiosonde data from 11 June. There are 5 stations, each with a sequence of 3 launchings. Cumulative integrated water content ("over-burden") at various pressure levels is shown versus launchtime. (A discussion of this display method is given in section 4.)
- Figure 4 shows the brightness temperatures computed from the 11 June radiosonde data using the computation method described by Kakar (1983).

b. Preliminary processing of measured and computed data

The measured and computed brightness temperatures were adjusted for two types of systematic error. The first affects the measured data; it is due to the variability in surface conditions. As explained below, the measured data set was normalized to a single reference ground pressure in an attempt to eliminate a part of this systematic error. The second adjustment affects the computed brightness temperatures; it was necessary to account for radiative transfer modeling inaccuracies and discrepancies between the measured and computed data due to systematic instrument effects. With the help of several coincident AMMS and radiosonde measurements, an average corrective bias temperature was obtained for each channel. These channel biases were added to the computed brightness temperatures to calibrate the computed data base. Since subtracting the biases from the measured values instead would be entirely equivalent, these two adjustments, viz. normalization of measured data and calibration of computed data, could have been combined as a single adjustment of the measured brightness temperatures without affecting the retrievals. We have dealt with them separately because of their different character, as discussed below in further detail.

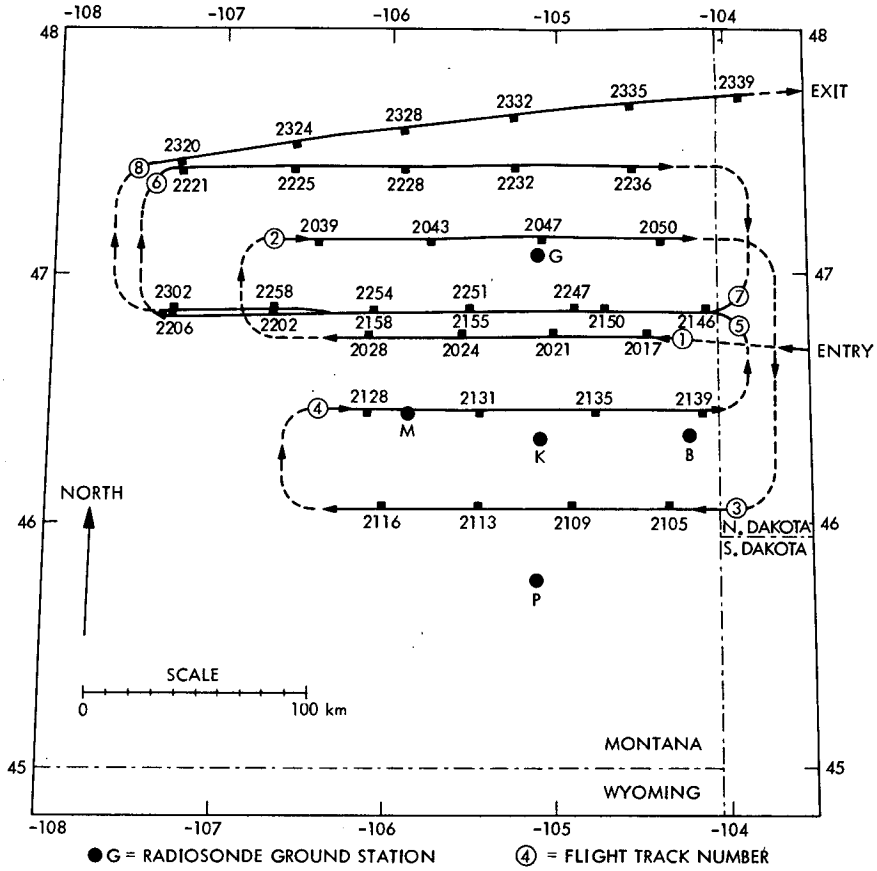

FIG. 1. CCOPE flight navigation map 11 June 1981. Stare mode sequences are indicated by tick marks and the time (GMT).

1) DATA NORMALIZATION

In order for the statistical retrieval method to function properly, it is necessary to ensure that the measurements reflect circumstances essentially similar to those used to generate the regression data base. That may require preliminary processing of the measured data, a step we shall refer to as data normalization. In particular, variability due to surface conditions, such as emissivity, elevation and temperature should as far as possible be eliminated. Implicit in the regression method is the assumption that a change in T_b is caused by a change in atmospheric conditions (e.g., moisture) and not by a change in surface properties.

Variability in the surface emissivity ϵ could be accommodated by including it in the data base. Thus, if it is expected that ϵ might vary from 0.95 to 0.99, the data base could be constructed using ϵ randomly distributed in this range. The price for the resulting broadening of the data base is, however, the introduction of an uncertainty, which will force the selection of only a small subset of channels as optimal and result in wide error margins for retrieved values. Equally wide error margins will result if the data base is constructed using a fixed ϵ and applied to unmodified T_b which correspond to actual ϵ which are different from the data base value. A solution is to generate the data base using some fixed emissivity, ascertaining the actual ϵ at each point, and normalizing the measured T_b to what would have been measured if ϵ had had that fixed value instead of the actual value.

Surface elevation variability has 3 consequences:

- the surface temperature T_s becomes variable because of a changing atmospheric temperature (assuming a normal temperature-profile, increasing elevation will result in decreasing T_s);
- the transmittance, τ, changes because of a variable amount of absorbing matter present in the radiation path (increasing elevation gives increasing τ);
- the atmospheric contribution, T_{atm}, to brightness temperature will change because of a changed amount of radiating matter present in the observation path (increasing elevation gives decreasing T_{atm}). The latter two effects will largely offset each other, however.

Over land, where ϵ is close to unity, the combined effect of variability in ϵ and T_s (the latter due to

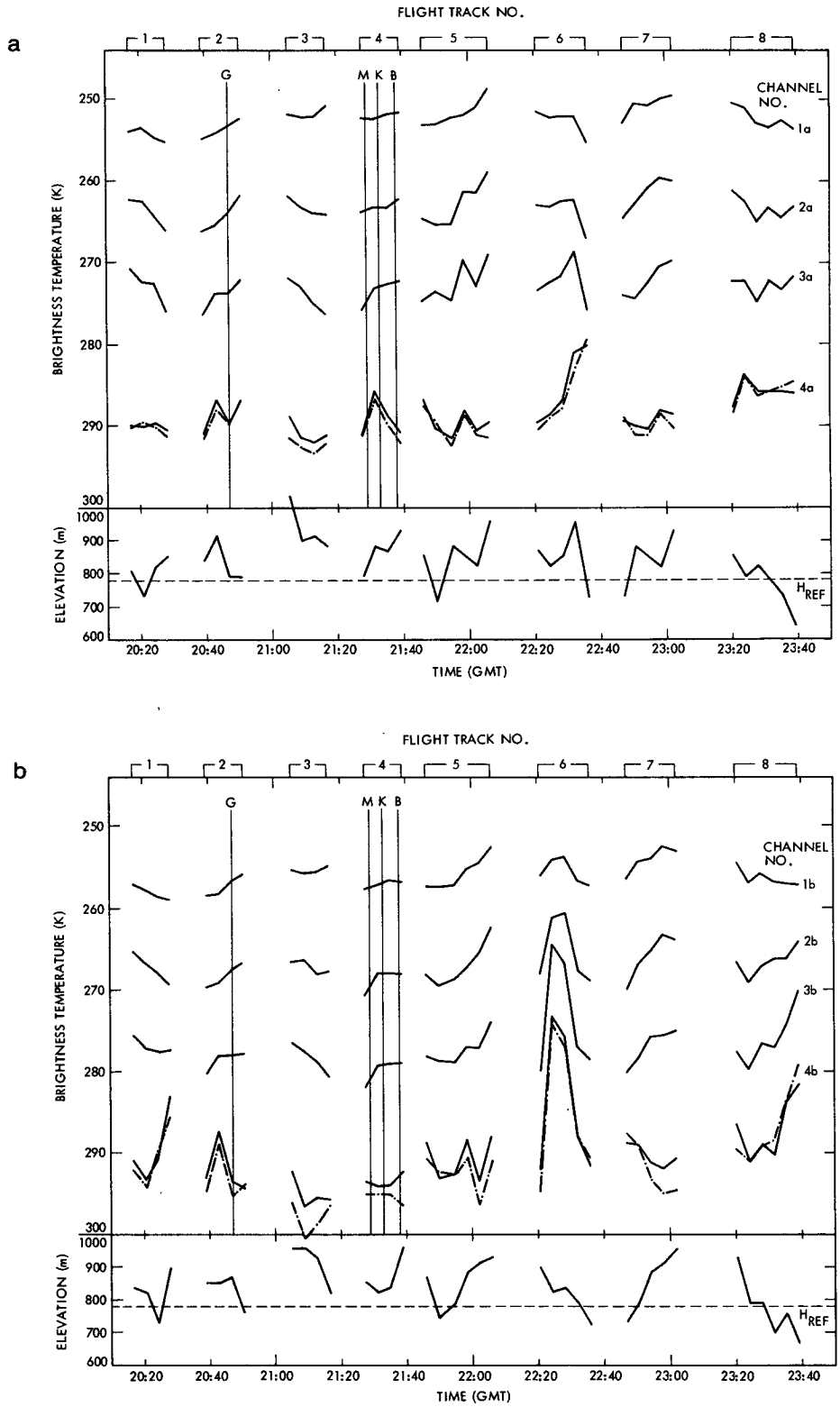

FIG. 2. 150-pixel averages of measured stare mode brightness temperatures, (a) at 45° right, (b) at nadir for 11 June 1981. Four vertical lines mark calibration points, each with the nearest radiosonde station indicated. The lower section shows ground elevation; the result of data normalization to a 782 m reference elevation is shown as broken lines for the window channels (4a, 4b).

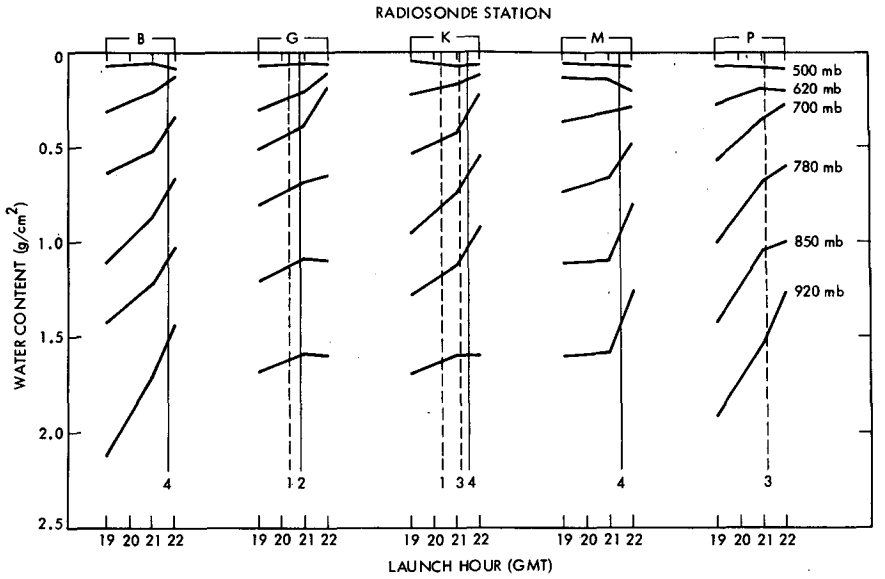

FIG. 3. Radiosonde moisture data (water content above various pressure levels), for three sondes from each of five stations. Vertical lines mark reference points, each labeled with the corresponding flight track number. Solid lines indicate primary references (no spatial interpolation), broken lines indicate secondary references (spatial interpolation required).

surface elevation only) can be expressed approximately as

$$\Delta T_b \approx \Delta(\epsilon T_s)\tau. \quad (2)$$

It is clear that, because of the transmittance factor, the window channel will be most affected, while the most absorptive channel will be least affected. Fur-

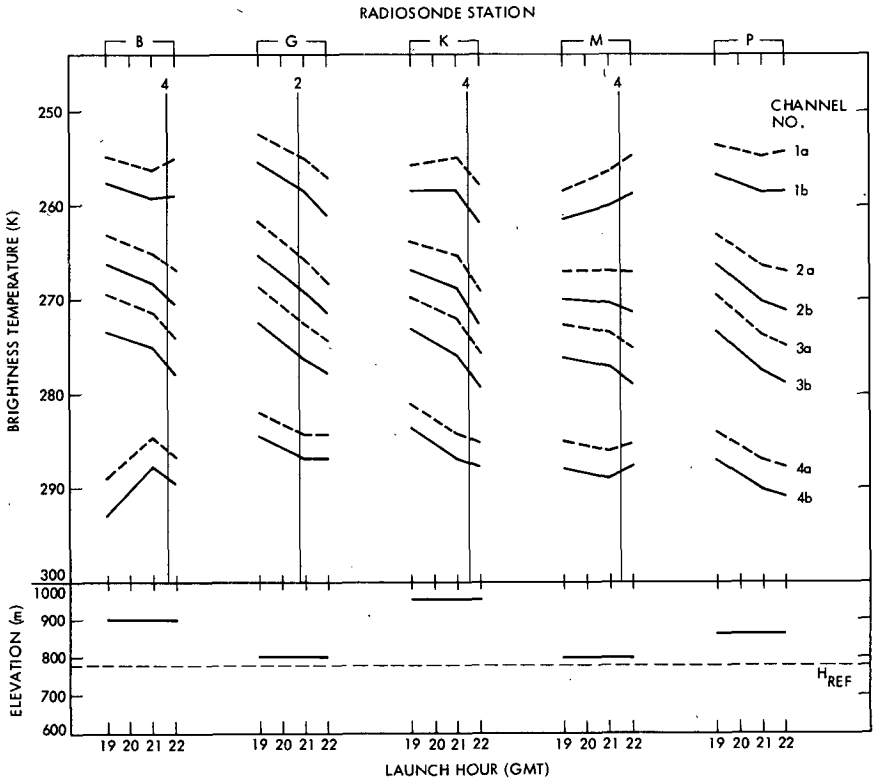

FIG. 4. Brightness temperatures computed from 11 June radiosonde data (Fig. 3). Four vertical lines mark calibration points, each labeled with the corresponding flight track number (cf. Fig. 2). The lower section shows the ground elevation at each radiosonde station.

thermore, nadir-looking measurements will be more affected than oblique measurements.

A couple of examples will serve to illustrate the importance of these effects. In the present case, i.e., CCOPE, the computed τ is typically 0.7 for the nadir-looking window channel, and T_s is of the order of 300 K. A fluctuation in ϵ of just 1% would then be equivalent to a ΔT_b of 2 K. A change in elevation of 100 m would be equivalent to a ΔT_b of another 2 K, if one assumes an atmospheric temperature lapse rate of 3 K/100 m (which there is reason to do, as will be discussed below). Thus, with the elevation variations shown in Fig. 2, it is quite conceivable that these two effects could be equivalent to an apparent random noise of 5–10 K in the window channel. This noise should be treated as systematic rather than random noise.

In practice, a complete normalization is a difficult task. Although we have been able to determine elevation (with an estimated uncertainty of 20–30 m), the atmospheric lapse rate and surface emissivity are difficult to ascertain. We have instead performed a linear regression analysis on elevation versus measured T_b for each channel in an attempt to determine the elevation gradient of a brightness temperature directly. The analysis, which is based on a sample size (i.e., stare mode locations) of 38, indicates a strong correlation between elevation and T_b for the nadir window channel and a weaker correlation for two other channels. The deduced gradients are listed in Table 1.

We chose 920 mb as the reference ground pressure, and determined from radiosonde ground data (interpolating with the adiabatic altitude-pressure function $H \sim p^{0.287}$) that the corresponding reference ground elevation on 11 June was 782 m—sea level pressure would then have been 1005 mb. (These figures will change with time, as they depend on the general atmospheric conditions in the area. Thus, during a low-pressure episode the 920 mb elevation will be low, while during a high-pressure episode it will be high.) The result of normalizing measured T_b to 782 m elevation is shown in detail in Fig. 2 for the window channel data and in summary in Table 1 for all channels. Average normalization correction applied to each channel is also shown in Table 1.

The deduced nadir window channel gradient of −2.2 K/100 m corresponds to an atmospheric lapse rate of 3.1 K/100 m if surface emissivity is assumed equal to 1. That may strike the reader as being improbably high, particularly compared to the 0.65 K/100 m lapse rate of the *1976 U.S. Standard Atmosphere* and the 1 K/100 m lapse rate of an isentropic atmosphere (Byers, 1959). However, in view of a critical auto-convective lapse rate (i.e., the minimum lapse rate which causes spontaneous convective flow) of 3.4 K/100 m (Byers, 1959), the figure is seen to be rather more likely, particularly given the circumstances under which our data was obtained. The 11 June CCOPE flights took place at midday during midsummer under partly clear skies and over mountainous terrain (presumably only sparsely covered by vegetation). Under such conditions one can expect substantial solar heating of the ground and consequent convection in the atmospheric boundary layer. It is thus quite likely that the lower atmosphere was not in thermodynamic equilibrium, and lapse rates even higher than the critical auto-convective rate are possible. In this light 3.1 K/100 m appears to be reasonable. Some of the CCOPE radiosondes also show evidence of a substantially increased lapse rate near ground.

We have limited our normalization efforts to the elevation normalization described here. We did not have sufficient data to separate the effects due to surface emissivity variation and the temperature lapse rate. Because of this partial data normalization, the effective noise in the window channels is still high. Our normalization thus consisted in, at every stare mode location, correcting each channel's measured T_b by the product of that channel's elevation gradient and the difference between that location's elevation and the reference elevation (782 m).

TABLE 1. Sensor channel characteristics, normalization of measured brightness temperatures and calibration of computed brightness temperatures.

Sensor channels				Normalization		Calibration
Channel	Freq. (GHz)	Angle (deg)	Typical τ	$\Delta T_b/\Delta H_s$* (K/100 m)	Avg. ΔT_b (K)	ΔT_b (K)
1a	183 ± 2	45	5×10^{-9}	0	0	−3.0
1b	183 ± 2	0	1×10^{-6}	0	0	−2.2
2a	183 ± 5	45	3×10^{-4}	0	0	−2.7
2b	183 ± 5	0	3×10^{-3}	0	0	−1.4
3a	183 ± 9	45	0.02	0	0	0.4
3b	183 ± 9	0	0.05	−0.5	−0.3	2.9
4a	92	45	0.6	−1.0	−0.6	4.9
4b	92	0	0.7	−2.2	−1.3	7.4

* Gradient of measured brightness temperature T_b vs surface elevation H_s, deduced from correlation analysis.

2) CALIBRATION

To calibrate computed T_b (i.e., compensate for computational errors) we have used five reference points. The navigation map, Fig. 1, shows that three of the radiosonde stations are situated on an east–west axis which nearly coincides with flight track 4. A simple time interpolation of the T_b values computed from these radiosondes, as shown in Fig. 4, then yields 3 sets of reference data which can be compared with three sets of time interpolated measured T_b from track 4, as indicated in Fig. 2. Similarly, one radiosonde station is near one of the data points of track 2. A time interpolation of the T_b values computed from those radiosondes again yields reference T_b which can be compared with the measured data from track 2, as marked in Fig. 2 and Fig. 4. Finally, T_b computed from the average 11 June radiosonde yields a reference which can be compared with the average clear-sky T_b measured on 11 June.

For each of the eight channels we can then determine an average "computation bias" from the five reference comparisons. (The bias is the difference between reference value and computed value.) The result is shown in Table 1. All computed brightness temperatures have been adjusted by the addition of these bias values.

3) OPTIMUM CHANNEL SUBSETS

To determine the optimal regression subsets we used the average 11 June radiosonde as the reference. Using, in turn, all best regression subsets (of size 1 through 8) derived from the statistical data base, to compute an average retrieved moisture profile and comparing with the reference profile at each pressure level, we selected the channel subsets listed in Table 2 as the best (i.e., yielding the best agreement for the average profile). Only $b_i(p)$ coefficients corresponding to the channels listed in Table 2 were used to retrieve the moisture profiles from the measured brightness temperatures by the application of Eq. (1). All other $b_i(p)$ coefficients were set equal to zero.

TABLE 2. Optimal sensor channel subsets.

Pressure (mb)	Best subset (channel number)
300	1a
350	1a
400	1a
430	1b
475	1b
500	3a
570	3b + 4a
620	3b + 4b
670	2b
700	3a
780	3b
850	3b
920	4b

Selection of only one channel for retrieval of moisture at most of the pressure levels is not an unexpected result. In an earlier simulation experiment (Kakar and Lambrigtsen, 1984), it was shown that two channels—corresponding to the peaks of the temperature weighting function and the water vapor contribution function (Kakar, 1983) respectively—were needed at most pressure levels for an optimum retrieval of tropical moisture profiles. This happened because additional channels contributed more noise than information to the retrieval process. It was also shown that if the temperature of the absorbing layer was assumed constant while the moisture content varied, then the brightness temperature of the moisture sensitive channel was negatively correlated with the moisture content of the absorbing layer. In other words, if the temperature profile did not vary much in a given region one moisture sensitive channel may be sufficient to retrieve specific humidity at most pressure levels.

4. Retrievals

Figure 5 shows the resulting retrieved moisture profiles. Water vapor mixing ratio as a function of pressure was found to be cumbersome to display because of frequent level crossovers; i.e., $q(p)$ for lower pressure became larger than at higher pressure, along the flight track. Therefore, we have opted to display water content, instead, in several fixed atmospheric layers in the form of cumulative integrated water content,

$$w(p_i) = \frac{1}{g}\int_0^{p_i} q(p')dp', \tag{3}$$

where $w(p_i)$ is a monotonic function and is also more smoothly varying than the corresponding $q(p_i)$. This display method permits easy visualization of both horizontal and vertical water vapor gradients. We chose to integrate down from $p = 0$ ("overburden"), rather than up from $p = 920$ mb ("underburden"), in order to minimize contamination of all but the last layer's w with the inevitable uncertainties arising from the surface effects and the only partially successful normalization efforts previously discussed. Thus, we believe the major uncertainty in w to be in the value at 920 mb; i.e., in total water content.

An inspection of the navigation map (Fig. 1) reveals that there are several locations where it is possible to check the validity and consistency of the retrievals.

- The 4 radiosonde stations which we used for calibration can also be used to check against retrievals. Time interpolation of the appropriate radiosonde moisture data (Fig. 3) yields the 4 reference profiles marked as "primary references" in Fig. 5. The agreement appears to be good but it should be kept in mind that the 920 mb w values (total water content) are fairly uncertain due to the uncertain ground

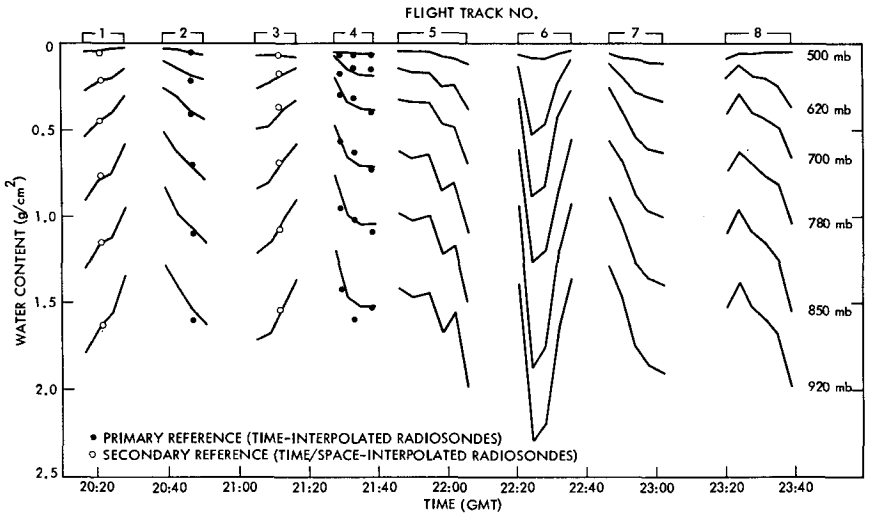

FIG. 5. Retrieved moisture data (water content above various pressure levels). The four "primary" reference profiles marked are identical to the primary reference points of Fig. 3. The two "secondary" reference profiles marked are spatial averages of the secondary reference points of Fig. 3.

normalization and the rather substantial extrapolation to 920 mb which some of the radiosondes have undergone. Furthermore, since the same reference data was used for calibration, one might expect good agreement. However, such calibration-induced agreement would apply to the averages used (i.e., the average of the 4 reference "radiosondes" and the 11 June average) and not necessarily to each reference point individually. Thus, although the result should be accepted with some caution, the comparison is a valid test.

• In addition, it is possible to derive further reference data by interpolating radiosondes spatially. Since such interpolation is rather uncertain, we have limited ourselves to a pair of simple cases where a flight track passes midway between two radiosonde stations (tracks 1 and 3). The two resultant reference profiles have been marked as "secondary references" in Fig. 5.

• It will also be noted that the retrieved horizontal gradient for track 4 agrees fairly well with that derived from the three radiosonde stations along track 4.

• Tracks 1 and 2 cover essentially the same area, with track 2 being 45 km north of track 1 and a little later in time. The retrievals give approximately the same east–west gradient for the two tracks.

• Similar circumstances pertain to tracks 3 and 4. Also there the gradients are quite similar. Furthermore, they agree with the gradients of tracks 1 and 2. Thus, all of tracks 1–4 agree that there was a substantial West-to-East moisture gradient of roughly 30% in w (or 0.5 g^{-2} cm^2 in total w) per 100 km during a time span of almost 1.5 hours.

• Tracks 5 and 7 are almost identical, but the latter occurred 1.5 hours after the former. Even so, the retrieved gradients agree fairly well with each other, but the resultant gradient is in the opposite direction of the one determined from tracks 1–4 (suggesting a substantial horizontal flow of moisture during the intervening time). The retrievals exhibit several other interesting features, such as the apparent moisture mass shown along track 6 (this may represent passage through a cloud—the latter were numerous during CCOPE). However, the scarcity of reference data (and the lack of radiosondes released after 2200 GMT) prohibits any meaningful comparisons on which to base any discussion.

5. Discussion

In evaluating our results, several factors which contribute to retrieval errors and uncertainty should be considered.

• Radiosondes do not represent instantaneous vertical soundings, but we have treated them as if they did. This would be especially important when large time gradients are present. Both regression data base and reference data used for calibration and optimization are affected.

• Only a very limited amount of reliable reference data is available, affecting calibration and optimization of the retrieval method and our ability to evaluate the results.

• Large gradients in time and space were present during CCOPE. This is problematic because we wish to reduce a three-dimensional time-dependent problem to a time sequence of one-dimensional problems; e.g., we have assumed that the atmosphere seen at 45° is the same as the one seen at nadir.

• Ground is at varying elevations and of unknown composition.

• The atmospheric temperature lapse rate near ground is uncertain.
• Thus, emissivity and surface temperatures are uncertain, which is equivalent to potentially substantial effective noise in measured brightness temperatures, particularly for window channels.
• Inaccuracies in the radiative-transfer computations, due to roundoff and truncation errors (inaccurate integration) and atmospheric modeling errors (inaccurate absorption coefficients), may not be fully compensated for through our calibration procedure. This affects the regression data base.

In order to reduce the effect of some of these uncertainties and improve the retrieval accuracy, it is recommended that in future experiments of a similar nature, some attention be paid to the following points:

1) If the surface emissivity can be ascertained at each data point, better data normalization can be achieved.
2) Data normalization can also be improved if the atmospheric temperature lapse rate near ground is determined. (It should be noted that the lapse rate may be substantially increased in a warm, convectively unstable boundary layer induced by solar heating of the surface. Such an effect would be a function of insolation; i.e., latitude, season and time of day and cloud cover, as well as surface emissivity particularly in the visible spectrum.)
3) By using simultaneous interpolation in time and one-dimensional space (altitude), each radiosonde can be properly treated as a time sequence of data. (In the present case, due to the north–south and east–west arrangement of the five radiosonde stations it would even be feasible to interpolate the radiosonde data in full four-dimensional space, so that reference data could be derived for any time and location. We have developed the necessary tools, but we decided against using them for the test described here, since it is doubtful that the sparse radiosonde data justifies the use of such sophisticated techniques.)

Acknowledgments. The authors are indebted to Dr. T. T. Wilheit of NASA/GSFC for making the CCOPE AMMS data available. We are also grateful to Dr. Joe Waters for making several helpful suggestions to improve the manuscript.

The research described in this paper was performed by the Jet Propulsion Laboratory, California Institute of Technology, under contract with the National Aeronautics and Space Administration.

REFERENCES

Byers, H. R., 1959: *General Meteorology,* McGraw-Hill, 540 pp.
Furnival, G. M., and R. W. Wilson, Jr., 1974: Regressions by leaps and bounds. *Technometrics,* **16,** 499–511.
Kakar, R. K., 1983: Retrieval of clear sky moisture profiles using the 183 GHz water vapor line. *J. Climate Appl. Meteor.,* **22,** 1282–1289.
——, and B. H. Lambrigtsen, 1984: A statistical correlation method for the retrieval of vertical moisture profiles by microwave radiometry. *J. Climate Appl. Meteor.,* **23,** 1110–1114.
Krupp, B. M., and R. A. Nieman, 1982: Observations with the Advanced Microwave Moisture Sounder (AMMS) during the 1981 Cooperative Convective Precipitation Experiment (CCOPE). Systems and Applied Sciences Corporation, Hyattsville, Maryland. Report for Contract NAS5-26753, 17 pp.